Crystal Fields in Metallic Magnetism

K. A. McEwen

Department of Physics, Birkbeck College, University of London,

Malet Street, London WC1E 7HX, UK

Abstract

The magnetic structure and excitations of praseodymium are reviewed. Two phenomena which cannot be understood within the standard model of rare earth magnetism are discussed. These are the quasielastic peak which is present in both the paramagnetic and antiferromagnetic phases, and the excitations which accompany the crystal field excitations near the Brillouin zone centre. We also review the properties of the localised moment compound UPd_3, and discuss the nature of the quadrupolar phases observed in this system.

1 Introduction

The crystal field interaction is an essential component of the standard model of rare earth magnetism, which Allan Mackintosh put forward. In this model, the $4f$ electrons are localised, with ground state multiplets determined by Hund's rules. Their magnetic moments interact with their surroundings through the single-ion crystalline electric field (CEF) interaction, which removes the degeneracy of the $|J, J_z\rangle$ ground multiplet. The f-electrons and the conduction electrons are weakly coupled, leading to the two-ion indirect RKKY exchange. Other interactions, such as the magnetoelastic and hyperfine interactions, and the classical dipolar couplings, are assumed to be relatively weak. A full account of the standard model and its application to the structures and excitations of the rare earths was given by Jens Jensen and Allan Mackintosh in their book (Jensen and Mackintosh, 1991), which reviews the field up to 1991.

CEF effects play a profound role in the magnetism of the light rare-earth metals, and in this paper I will examine new results which have been discovered since 1991. Some of these results provide a stringent test for the standard model, and suggest that the model breaks down when the coupling with the conduction electrons becomes sufficiently strong that the $4f$ states develop a significant band-like component. Indeed Allan Mackintosh recognised this effect was central to an understanding of cerium, which he called a $4f$ band metal (Mackintosh, 1985). I shall

also discuss some actinide compounds in which clear evidence for localised moment magnetism and CEF effects have been observed.

2 Praseodymium

Pr is in many respects the apotheosis of the standard model of rare earth magnetism: although it has been extensively studied for many years, new aspects of its magnetic behaviour have been discovered in the past five years. In particular, there are now two well-established phenomena which cannot be understood within the standard model, and we shall discuss them in some detail, after a brief outline of the essential properties of this element.

The crystal structure of Pr is double-hexagonal close-packed, with locally hexagonal and cubic sites. The first model for the CEF splitting of the $4f^2, J = 4$ ground multiplet, was put forward by Bleaney (1963), based on heat capacity and susceptibility data from polycrystalline samples. Singlet ground states at both sites were proposed. With the advent of single crystals in the 1970s, the magnetic excitations and bulk properties (magnetisation, susceptibility) were studied. The level scheme of Rainford and Houmann (1971), subsequently refined by Jensen (1979), accounts well for the observed properties. On the hexagonal sites, the ground state is $|J_z = 0\rangle$ with the first excited (doublet) states of $|J_z = \pm 1\rangle$ at 3.5 meV. On the cubic sites the ground state is also a singlet separated by 7.5 meV from the excited Γ_4 triplet. The overall splitting of the $J = 4$ multiplet is about 15 meV. This level scheme accounts for a large anisotropy of the moments on the hexagonal sites in a magnetic field. At low temperatures, there is thus no moment induced on the hexagonal sites by a field along the c-axis until the Zeeman splitting brings about a level crossing of one of the excited states with the singlet state. Such a metamagnetic transition, resulting in a large increase in the magnetisation, was found by McEwen et al. (1973) to take place at 32 tesla.

The criterion for magnetic ordering in a singlet ground state system may be easily seen from the inverse magnetic susceptibility in a mean field approximation:

$$\chi^{-1}(\boldsymbol{q}) = \left[\frac{2g^2\mu_B^2\alpha^2}{\Delta}\right]^{-1} - \mathcal{J}(\boldsymbol{q})$$

where Δ is the energy gap between the ground and first excited CEF state, and α is the matrix element $\langle e|J_\xi|g\rangle$ connecting them. The criterion for the divergence of χ^{-1} and hence magnetic ordering is

$$\frac{2\mathcal{J}(\boldsymbol{q})g^2\mu_B^2\alpha^2}{\Delta} \geq 1$$

i.e. the exchange energy divided by the crystal field splitting must exceed a critical ratio. A comprehensive study of the magnetic excitations in Pr at 6 K was carried out at Risø by Houmann, Rainford, Jensen and Mackintosh in the 1970s. Their measurements (Houmann et al., 1979) revealed a strong dispersion of the crystal field excitations (called magnetic excitons) with a well defined minimum along the ΓM direction. From the energy of this incipient soft mode, it was deduced that the exchange is some 92% of the critical value for ordering.

Magnetic ordering in Pr thus requires either a reduction in the CF splitting (Δ) or an increase in the exchange $J(\boldsymbol{Q})$. Jensen's suggestion that a suitably applied uniaxial stress might induce ordering in Pr was exhaustively investigated by McEwen, Stirling and Vettier in experiments (McEwen et al., 1978, 1983a, 1983b) at the ILL. These demonstrated that only a very modest uniaxial pressure, e.g. 1 kbar (100 MPa), along the a-axis is required to split the excited doublet and produce a large ordered moment ($\approx 1\ \mu_B$). In the pressure-induced magnetic structure the moments are longitudinally polarised along the real-space b direction in an incommensurable structure whose wave vector is $\boldsymbol{q} = 0.13\boldsymbol{\tau}_{100}$, and are also coupled antiferromagnetically along the c-axis. Under pressure, the excitations showed a pronounced softening, and became overdamped around the critical wave vector (Jensen et al., 1987).

Magnetic ordering in Pr may also be produced by another mechanism, via the hyperfine coupling. Since the nuclear spin of Pr (which exists naturally only as the single isotope ^{141}Pr) is $I = \frac{5}{2}$, the Curie susceptibility of the nuclear spins will diverge at sufficiently low temperatures and the coupling $A\,\boldsymbol{I} \cdot \boldsymbol{S}$ to the electronic moments will eventually lead to their order, as predicted by Murao (1971, 1975, 1979). Experiments at ILL (McEwen and Stirling, 1981) and Risø (Bjerrum Møller et al., 1982) in the 1980s demonstrated this effect in principle, but cryogenic difficulties restricted the range of the measurements to just below the Néel temperature of $T_N \approx 50$ mK.

The onset of magnetic ordering in Pr is, however, most unusual. Already at temperatures far above T_N, fluctuations appear at a wave vector of $\boldsymbol{q}_1 = 0.105\boldsymbol{\tau}_{100}$, as seen in the neutron scattering data shown in Fig. 1. These fluctuations grow as the temperature is reduced, and then a second peak appears at $\boldsymbol{q}_2 = 0.13\boldsymbol{\tau}_{100}$. It is this latter peak which is eventually the signature of the long-range order, but the first peak continues to grow, albeit at a slower rate, and coexists in the ordered phase. Its q-width is greater than the experimental resolution so it is not truly long range: it is known as the broad, central or quasielastic peak, and it cannot easily be understood within the standard model. The coexistence in the ordered phase of a resolution limited magnetic satellite peak at one wave vector, and a broader peak at a different wave vector is a phenomenon unique to Pr.

More recently, we have extended these studies to temperatures well below T_N

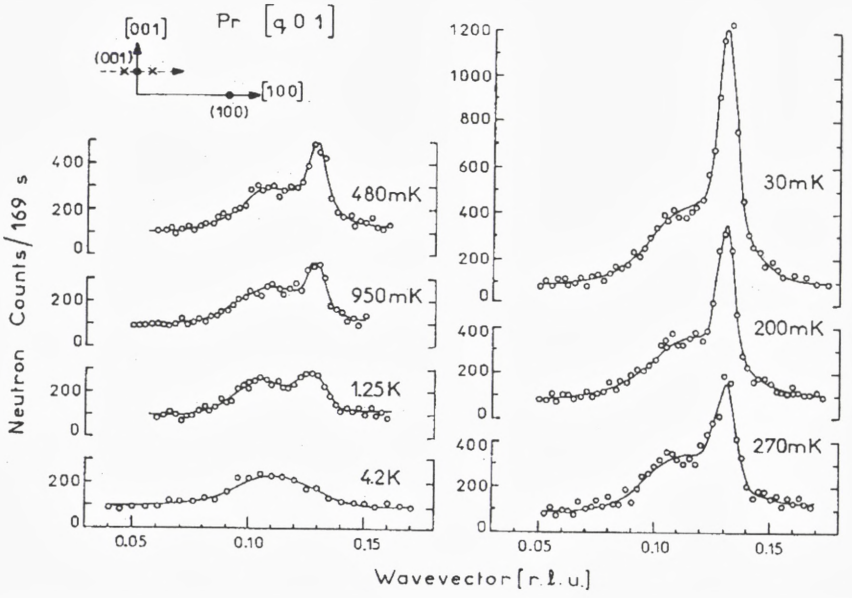

Figure 1. Elastic neutron scattering scans through $(q, 0, 1)$ in Pr as a function of temperature, measured on the IN2 spectrometer at the ILL, Grenoble, from McEwen and Stirling (1981). The data have been fitted to two gaussians. It is now clear that the lowest sample temperature was significantly above 30 mK.

in a collaboration with the group at HMI Berlin, and have succeeded in carrying out both elastic and inelastic neutron scattering measurements on Pr at temperatures down to 9 mK (Moolenaar et al., 1997). We have confirmed that the central peak coexists with the satellite peak in the truly long-range ordered phase, and were at last able to measure the saturation intensities of the magnetic satellite and central peaks. Figure 2 shows elastic scattering scans through the $(q, 0, 3)$ position, which may be directly compared with the earlier ILL data. We see that at 175 mK, the broad peak is centred around $\boldsymbol{q}_1 = 0.105\boldsymbol{\tau}_{100}$, as in Fig. 1, although it is clear that this part of the scattering function is not particularly well modelled by a single Gaussian, and the satellite peak is centred at $\boldsymbol{q}_2 = 0.13\boldsymbol{\tau}_{100}$. However, at lower temperatures, the broad peak component is best fitted by a Gaussian function whose centre moves steadily towards the satellite wave vector, which remains essentially fixed at $0.13\boldsymbol{\tau}_{100}$.

Figure 3 presents the temperature dependence of the ratio of the integrated intensity of the $(q_2, 0, 1)$ and $(q_2, 0, 3)$ magnetic satellite peaks, normalised to the intensity of the $(1, 0, 0)$ nuclear Bragg reflection. There is good agreement between

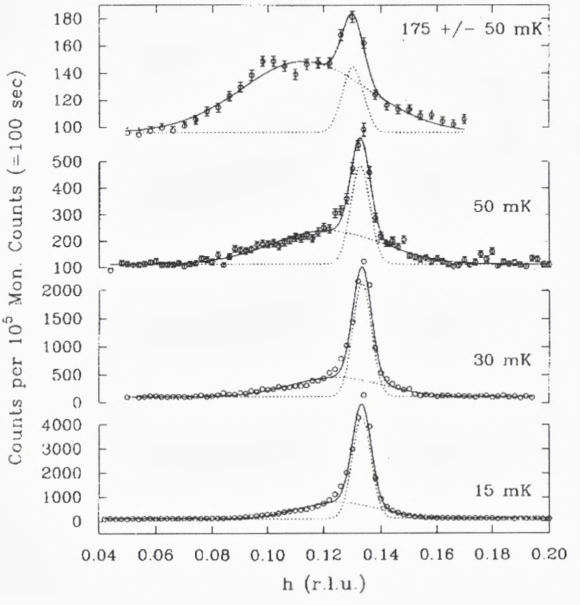

Figure 2. Elastic neutron scattering scans through $(q, 0, 3)$ in Pr as a function of temperature, measured on the V2 spectrometer at the HMI, Berlin, from Moolenaar et al. (1997). The data have been fitted to two gaussians.

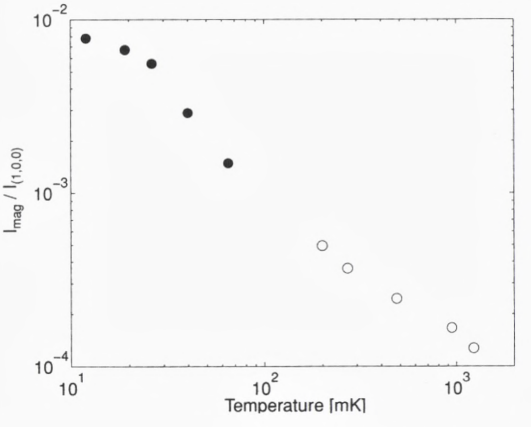

Figure 3. Temperature dependence of the integrated intensity of the satellite peaks at $(q_2, 0, 1)$ and $(q_2, 0, 3)$, normalised to the intensity of the $(1, 0, 0)$ Bragg peak, from the data of (o) McEwen and Stirling (1981) and (•) Moolenaar et al. (1997).

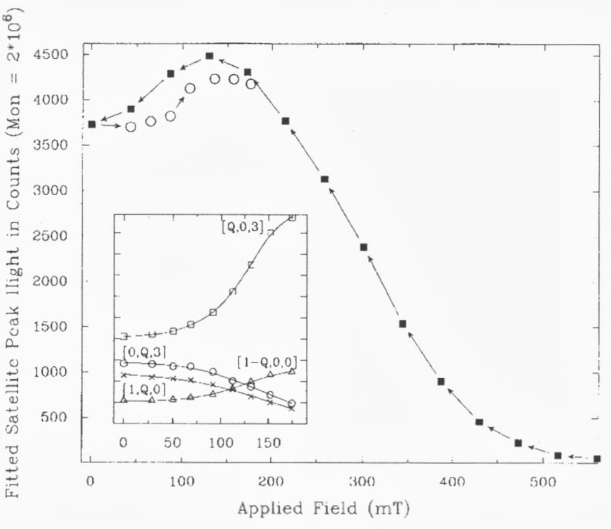

Figure 4. The magnetic field dependence of the in-plane and out-of-plane satellites in Pr, measured at $T = 10$ mK, on the V1 diffractometer at the HMI, Berlin, from Moolenaar et al. (1997).

the measurements at HMI and at ILL, which were made 15 years apart. We deduce the saturation moment to be $0.54 \pm 0.1\ \mu_B$, assuming that the magnetic structure comprises three equally populated domains. This is in reasonably good agreement with the $T = 0$ moment of $0.6\ \mu_B$, calculated by Jensen (Jensen and Mackintosh, 1991).

The magnetic structure may be described by

$$\boldsymbol{m}(\boldsymbol{r}_i) = m_{\|}\hat{\boldsymbol{b}}\sin(\boldsymbol{Q}\cdot\boldsymbol{r}_i + \phi_b) + m_{\perp}\hat{\boldsymbol{a}}\sin(\boldsymbol{Q}\cdot\boldsymbol{r}_i + \phi_a)$$

where $m_{\|}$ denotes a moment parallel to one of the three real-space b directions ([100] in reciprocal space), and $m_{\perp}$ is a moment along the perpendicular a direction. The ordering wave vector $\boldsymbol{Q}$ is that of the magnetic satellites, i.e. $\boldsymbol{q}_2 = 0.13\boldsymbol{\tau}_{100}$.

The results discussed above have shown that the intensity of the broad peak follows that of the satellite peak, as a function of temperature. A particularly interesting new result was the discovery that the magnetic field dependence of the two peaks differs. In the experimental configuration used for these studies, the Pr single crystal was mounted with (real-space) b and c directions in the horizontal scattering plane of the neutron spectrometer. In this way, diffraction peaks from one domain of the magnetic structure lie in the scattering plane (the *in-plane satellites*). The magnetic moments of the other two domains lie at $\pm 60°$ out of the horizontal plane, but some of their diffraction peaks (the *out-of-plane satellites*)

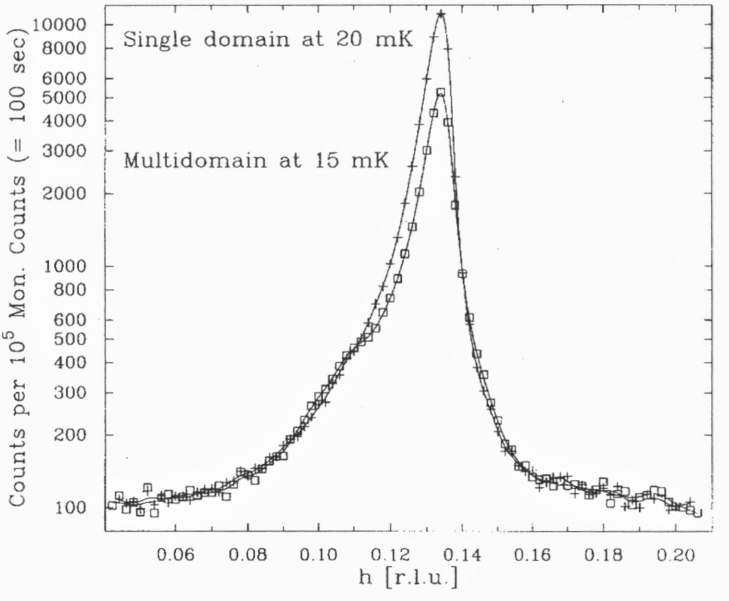

Figure 5. Comparison of $(q, 0, 3)$ scans for Pr at $T = 15$ mK, prepared in the multi-domain (zero-field cooled) and single-domain (field cooled) states, from Moolenaar et al. (1997).

may nevertheless be accessed by an appropriate tilt of the cryostat or the detector. With the sample at a temperature well below T_N, a magnetic field was applied in the vertical direction selecting, as expected for an antiferromagnet (see, for example, McEwen and Walker, 1986), the domain for which the magnetic moments were perpendicular to the field. Figure 4 shows the consequent increase in intensity of the in-plane satellite reflection, and the concomitant decrease of the out-of-plane reflections. At 10 mK, a field of 0.2 tesla suffices to produce a single domain structure. A single domain phase can also be prepared by cooling the sample through T_N in a magnetic field and then reducing the field to zero. Figure 5 illustrates the results of a $(q, 0, 3)$ scan for the single domain sample of Pr at 15 mK, prepared by field cooling, together with a similar scan for the multi-domain state, measured after the sample had been cooled in zero field. Whilst the satellite component has an intensity in the single domain state close to three times that of the multi-domain sample, as expected, the intensity of the broad peak component is clearly the same in both the single domain and multi-domain cases. This result is undoubtedly significant, and requires further theoretical understanding.

The field dependence shows that a field in the basal plane leads to a rapid

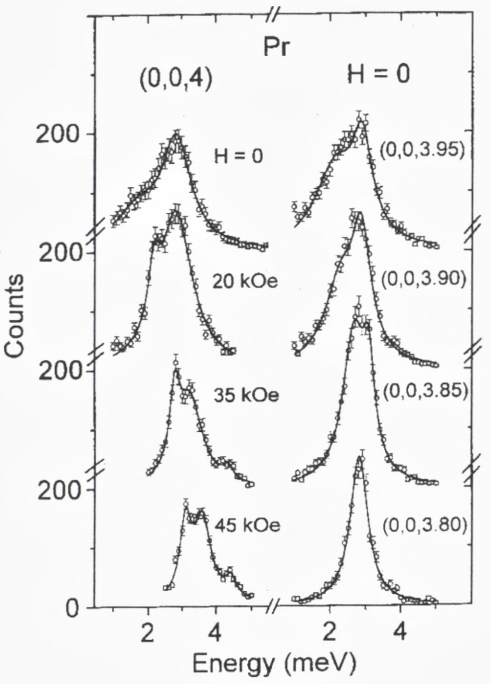

Figure 6. Inelastic neutron scattering spectra for Pr at $T = 4.2$ K, for wavevectors from $(0,0,4)$ to $(0,0,3.80)$, measured on the TAS7 spectrometer at Risø, from (Clausen et al., 1994a, 1994bb). The data have been fitted to Lorentzian functions convoluted with the experimental resolution.

reduction in satellite intensity. At 10 mK the magnetic moment is quenched in a applied field of 0.5 T. The effect of the magnetic field is twofold. Firstly the energy of the crystal field excitations is increased slightly, leading to a reduction in the ratio of exchange to crystal field splitting. The second effect is more significant: the nuclear moments are strongly polarised by the applied field since the effective field seen by the nuclei is enhanced by a factor of about 40 (see p. 351 of Jensen and Mackintosh, 1991). Due to this strong polarisation the susceptibility of the nuclear moments is substantially reduced. The combined effect of these factors is to reduce T_N to below 10 mK and hence the satellite intensity due to long range order disappears.

Another feature of Pr which cannot be understood within the standard model was discovered in a series of experiments at Risø which were carried out shortly after the redevelopment of the cold neutron guide produced a major increase in the neutron flux at the triple-axis spectrometer TAS7. In the paramagnetic phase, the

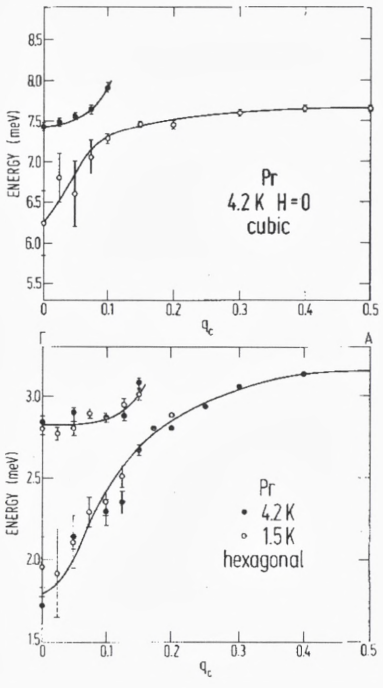

Figure 7. Dispersion relations for the magnetic excitations in Pr in the c-direction, as a function of q in units of τ_{001}, from (Clausen et al., 1994a, 1994b). For both the cubic and hexagonal sites, a lower energy *satellite excitation* hybridizes with the single branch of crystal field excitations predicted by the standard model.

crystal field excitations (magnetic excitons) broaden at wave vectors q approaching the zone centre, as was first reported by Houmann et al. (1979), and discussed in Jensen and Mackintosh (1991). This broadening is most easily observed along the c-direction, where the standard model predicts only one mode on each of the hexagonal and cubic sites. However, a careful study of the linewidths of these excitations at 4.2 K, made after the flux increase, revealed evidence of a second mode, as shown in Fig. 6, for wave vectors from $q = 0$ to $q = 0.15$ (Clausen et al., 1994a, 1994b). This second mode (the mode has been named a "satellite excitation", but this name is a source of potential confusion, since the mode is not directly linked to the elastic satellite peaks) appears to have an energy of 1.0 meV less than the $4f$ mode at the zone centre, but rises rapidly to hybridise with it. Similar behaviour was found around $q = 0$ for the cubic site excitations. The relevant dispersion relations are illustrated in Fig. 7.

Measurements of these excitations in a field along the a-axis showed that their

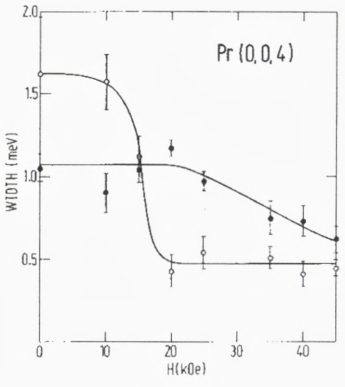

Figure 8. Magnetic field dependence of the width of the hexagonal site excitations in Pr at $(0, 0, 4)$, from (Clausen et al., 1994a, 1994b). The open circles correspond to the lower branch (satellite excitation) in Fig. 7, and the closed circles to the upper branch (standard model crystal field excitation).

width is rapidly reduced in an applied magnetic field (Clausen et al., 1994a, 1994b). In particular the width of the lower energy excitation shows a sharp drop between 1 and 2 tesla (see Fig. 8). It is interesting to note that this corresponds to the magnetic field at which the central peak is quenched (see Fig. 9).

Neither the broad peak observed close to the magnetic satellite wave vector, nor the extra excitations found in the paramagnetic phase of Pr can be explained within the standard model of rare-earth magnetism. The most plausible explanation for these phenomena is that they have their origin in a hybridization of the $4f$ electrons and the conduction electron states: a calculation of $\chi(\boldsymbol{q}, \omega)$ with this hybridization is therefore required, and we hope that our experiments will stimulate further progress in this direction.

3 Crystal fields in the actinides

The standard model developed for the rare-earth metals cannot be generally applied to the interpretation of the magnetism of the actinides. The strong *spd–f* hybridization present in these materials means that the basic assumption of the standard model, of localised moments and conduction electrons relatively weakly coupled to them, is not normally valid. However, there are a small number of actinide compounds which do exhibit a good approximation to localised moment magnetism and it is interesting to examine how far the standard model can be applied in these cases. One particularly important example of such a system is the uranium intermetallic compound UPd_3.

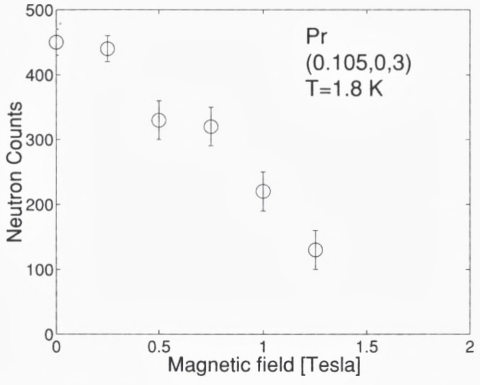

Figure 9. Magnetic field dependence of the intensity of the broad peak in Pr at $\boldsymbol{q}_1 = 0.105\boldsymbol{\tau}_{100}$, measured in the paramagnetic phase at 1.8 K.

3.1 UPd_3

Like Pr, the crystal structure of UPd_3 is double-hexagonal close-packed. The electronic configuration is $5f^2$, as confirmed by the intermultiplet transitions observed in high energy neutron spectroscopy (Bull et al., 1996). The peak at 380 meV is attributed to transitions from the $^3H_4$ ground multiplet to the excited $^3F_2$ multiplet. This result may be compared with the heavy-fermion compound UPt_3, where inelastic neutron spectroscopy showed the equivalent transition to be very much weaker, as expected due to the band-like character of its $5f$ electrons. Magnetic excitations at lower energies (1–20 meV) were first observed in UPd_3 by Buyers and Holden (1985) who interpreted them as crystal field excitations. As in the case of Pr, there appear to be singlet ground states on both the hexagonal and cubic site ions, but in contrast to Pr, the higher lying modes (at 15–20 meV) arise from transitions on the hexagonal sites, whilst the modes at 1–3 meV originate on the cubic sites. The overall splitting of the ground multiplet is some 40 meV, considerably greater than found in Pr or other rare-earths.

The presence of at least two phase transitions in UPd_3 has been known for some time: heat capacity (Andres et al., 1978) and thermal expansion measurements (Ott et al., 1980) indicated transitions around 7K and 5K. More recent thermal expansion (Zochowski and McEwen, 1994) and magnetization (McEwen et al., 1994; Park and McEwen, 1997) measurements on single crystals have confirmed these transitions and revealed the existence of a third transition near 8 K.

The magnetic susceptibility of the hexagonal and cubic site ions may be determined separately, by polarised neutron diffraction measurements in a magnetic field. Figure 10 shows the magnetic moment on the two uranium sites of UPd_3, in

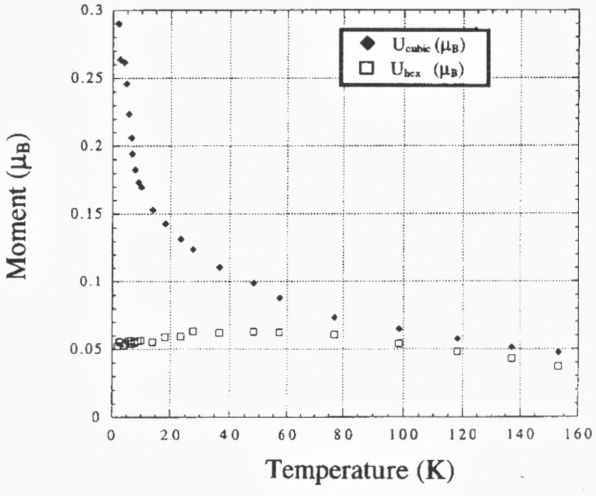

Figure 10. Magnetic moment on the hexagonal and cubic sites in UPd_3 in a field of 4.6 T along the a-axis, as a function of temperature, measured on the D3 diffractometer at the ILL, from Park et al. (1997).

a field of 4.6 tesla along the a-axis, measured with the D3 diffractometer at the ILL (Park et al., 1997). The anisotropy between the two sites is striking: whilst the moment on the hexagonal sites varies little below 100 K, the cubic site moment increases steadily as the temperature is reduced. This behaviour of the moments can be understood within the crystal field scheme described above. The relatively small values of the magnetic moments (particularly on the hexagonal sites) means that it is not practical to determine accurately the details of the moment variations on the two sites near phase transitions. However, the bulk magnetization measurements on UPd_3 single crystals, shown in Fig. 11 (McEwen et al., 1994) clearly reveal the phase transitions at $T_1 = 7$ K and $T_2 = 4.5$ K in the measurements for fields along the a-, b- and c- axes.

In their early neutron diffraction experiments at Chalk River, Buyers and Holden (1985) discovered new reflections below T_1 at positions $\left(h + \frac{1}{2}, 0, \ell\right)$ in reciprocal space. Subsequently, Steigenberger et al. (1992) carried out a more detailed investigation, using polarised neutron diffraction techniques. They found that the temperature dependence of reflections such as $\left(\frac{1}{2}, 0, 3\right)$ and $\left(\frac{1}{2}, 0, 4\right)$ also showed anomalies at the transition at T_2. Most significant was the finding that the scattering cross-section for these superlattice reflections was *non-spin-flip*, demonstrating that their origin was structural, rather than magnetic.

This result indicates that the primary order parameter is quadrupolar. It is the

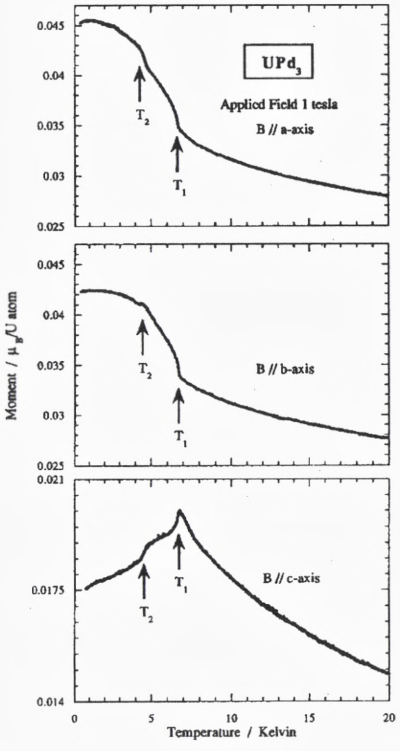

Figure 11. Magnetization of UPd_3 in a field of 1 T applied along the a-, b- and c-axes, from McEwen et al. (1994).

periodic lattice distortions produced by the ordering of the quadrupolar moments which couple to neutrons and give rise to the superlattice reflections. The development of quadrupolar ordering is consistent with a crystal field model for UPd_3 in which the ground states at both the hexagonal and cubic sites are singlets. Each uranium ion may have, in general, five independent quadrupole moments which we denote by Q_{zz}, $Q_{x^2-y^2}$, Q_{xy}, Q_{yz} and Q_{zx}. Above the ordering temperature, the only quadrupole moment which has a non-zero expectation value is Q_{zz}. With four uranium ions per unit cell in the dhcp crystal structure, there are 20 linearly independent quadrupolar symmetry modes. The group theory analysis of Walker et al. (1994) showed that this permits 8 possible order parameters. By comparing the observed intensities of the $\left(h+\frac{1}{2},0,\ell\right)$ superlattice reflections with those expected for the possible order parameters, it was deduced that the order parameter has B_{2g} symmetry. The doubling of the unit cell means that the structure is, of course, antiferroquadrupolar (AFQ), and B_{2g} symmetry implies that the possible

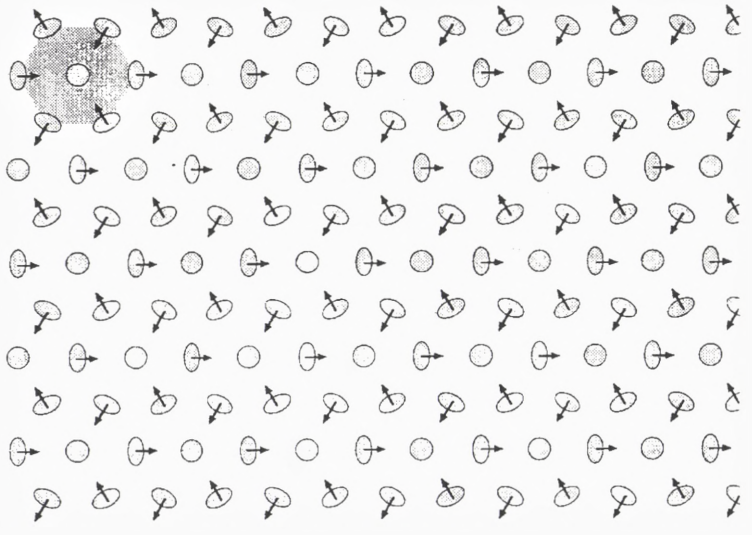

Figure 12. The antiferroquadrupolar structure of UPd_3, as described in the text.

components of the structure are a combination of $Q_{x^2-y^2}$, Q_{zx} and Q_{zz} quadrupolar moments on the cubic sites and Q_{zz} quadrupolar moments on the hexagonal sites. The presence of weak reflections at $\left(\frac{1}{2}, 0, 0\right)$ was attributed to the structure being triple-q, and the AFQ structure is illustrated in Fig. 12. In this figure, the shaded ellipsoids represent the charge densities of the $5f^2$ electrons at the uranium sites, for a section of the basal plane. The doubling of the chemical unit cell and the triple-q nature of the structure are obvious. The arrows do not denote dipolar moments, which are of course absent in this phase, but indicate the direction about which the charge densities are tilted out of the basal plane to produce Q_{zx} components. The charge densities without arrows are not spherical, but rather are spheroidal due to the Q_{zz} component.

The magnetic phase diagrams for UPd_3 have been deduced from thermal expansion measurements made in constant magnetic fields (Zochowski and McEwen, 1994) and magnetization studies (McEwen et al., 1994; Park et al., 1997). It is now clear that there exist three transitions, at temperatures (in zero magnetic field) of 7.8 ± 0.2 K, 6.8 ± 0.1 K and 4.4 ± 0.1 K. We shall denote these temperatures by T_0, T_1 and T_2, respectively. The transition at T_0 is most apparent in the thermal expansion (Zochowski and McEwen, 1994) but careful examination shows it is present also in the susceptibility data (Park and McEwen, 1997). A re-examination of the neutron scattering data published in Steigenberger et al. (1992), confirmed in more recent measurements, reveals that the $\left(\frac{1}{2}, 0, 3\right)$ peak appears at a higher

temperature than the $\left(\frac{1}{2}, 0, 4\right)$ peak. The magnetic field dependence of the three

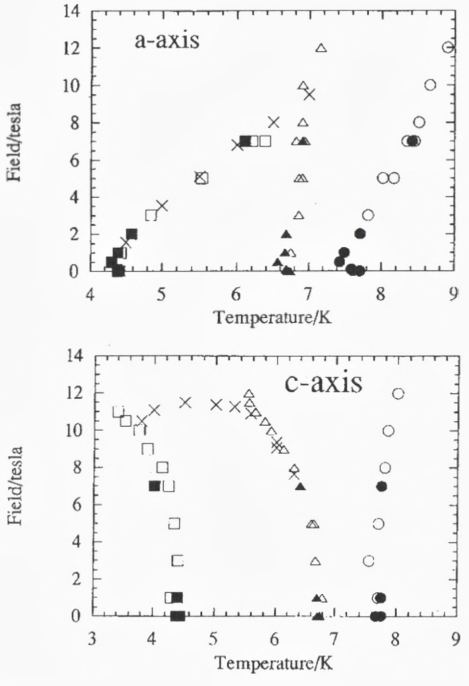

Figure 13. Magnetic phase diagrams of UPd_3 for fields along the a-axis and c-axis, from (Park and McEwen, 1997).

transition temperatures has been mapped out by following the anomalies associated with each of them. Figure 13 shows the phase diagrams for fields along the a-axis and c-axis (Park and McEwen, 1997).

Having mapped out the phase diagrams by macroscopic measurement techniques, we have begun to investigate them by neutron diffraction studies in a magnetic field. Figure 14 shows measurements made at Risø of the temperature dependence of the $\left(\frac{1}{2}, 0, 1\right)$ and $\left(\frac{1}{2}, 0, 2\right)$ peaks for UPd_3 in a field of 4 tesla applied along the vertical a-axis perpendicular to the horizontal scattering plane McEwen et al. (1997). It is clear that the scattering at $\left(\frac{1}{2}, 0, 1\right)$ develops below T_0, with a small but distinct anomaly at T_1, whereas the much less intense $\left(\frac{1}{2}, 0, 2\right)$ peak develops only below T_1. The intensity of this latter peak drops precipitously at T_2, as shown in the figure.

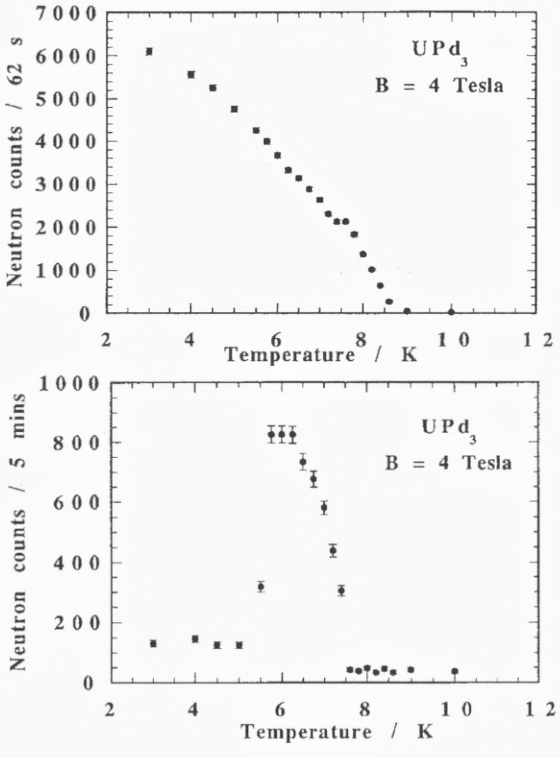

Figure 14. Temperature dependence of the $\left(\frac{1}{2},0,1\right)$ and $\left(\frac{1}{2},0,2\right)$ reflections in UPd_3 in a field of 4 T applied along the a-axis perpendicular to the scattering plane, measured on the TAS7 spectrometer at Risø, from McEwen et al. (1997).

The intensities of these reflections in a magnetic field are greatly enhanced over their zero field values, indicating the presence of magnetic scattering in this case. Again we have employed polarised neutrons to determine the origin of the superlattice reflections. Experiments at ILL have demonstrated that the $\left(\frac{1}{2},0,1\right)$ scattering between T_0 and T_1 is entirely *non-spin-flip* (Steigenberger et al., 1997). In the experimental configuration used (which was as for the measurements shown in Fig. 14), this result implies that the neutron scattering for $T_0 > T > T_1$ may arise both from structural components and from magnetic moments parallel to the direction of the neutron polarisation (i.e. the a-axis direction of the magnetic field). Since the intensity of the $\left(\frac{1}{2},0,1\right)$ reflection is so much greater than in zero field, where it is due to the structural distortion only, we may deduce that the magnetic field has induced a *ferrimagnetic* structure with the moments parallel to the field direction. When an a-axis magnetic field is applied to a quadrupolar structure of

symmetry B_{2g}, the induced magnetic structure is expected to have A_g symmetry (Walker, private communication), and a detailed analysis of the diffraction data confirms that this is indeed the case.

As mentioned earlier, UPd_3 is a rare example of a metallic actinide system for which well-defined magnetic excitations have been observed, and this evidence provides important justification for using a crystal field model to interpret its magnetic properties. The excitations with energies in the 1–3 meV range arise from crystal field transitions propagating on the cubic sites. Their dispersion and temperature dependence through the phase transitions has been studied (McEwen et al., 1993).

In our consideration of uranium compounds, we have concentrated on UPd_3. However, it should be noted that crystal field effects have been considered in a few other uranium intermetallic compounds. The system $U_xY_{1-x}Pd_3$ has attracted much attention because of its non-Fermi liquid behaviour for compositions near $x = 0.2$. However, clear evidence for crystal field like excitations at energies of 2–5 meV and 36–40 meV has been found in $U_{0.45}Y_{0.55}Pd_3$, and the evolution of these with uranium composition has been studied (McEwen et al., 1995). Another system in which crystal field excitations have been observed is the heavy fermion compound URu_2Si_2 (Broholm et al., 1987, 1991). The nature of the order parameter at the 17.5 K phase transition in URu_2Si_2 is the subject of current investigation by several groups. A crystal field model has been employed (Santini and Amoretti, 1994) to understand the transition but this explanation remains controversial.

4 Acknowledgements

This paper is dedicated to the memory of Allan Mackintosh, who introduced me to the fascinating properties of the rare earths. I greatly valued his friendship and collaboration over many years: his deep understanding and physical insight was a constant source of inspiration. I am also most grateful to my many collaborators and co-authors in the work reported here: special thanks go to Jens Jensen, Kurt Clausen and Uschi Steigenberger. This research has been financially supported by the UK Engineering and Physical Sciences Research Council and by the HCM and TMR Large Scale Facilities Programmes of the European Commission.

References

Andres K, Davidov D, Dernier P, Hsu F, Reed WA and Nieuwenhuys GJ, 1978: Solid State Commun. **28**, 405

Bjerrum Møller H, Jensen JZ, Wulff M, Mackintosh AR, McMasters OD and Gschneidner Jnr KA, 1982: Phys. Rev. Lett. **49**, 482

Bleaney B, 1963: Proc. Roy. Soc. A **276** 39

Broholm C, Kjems JK, Buyers WJL, Matthews PT, Palstra TTM, Menovsky AA and Mydosh JA, 1987: Phys. Rev. Lett. **58**, 1467

Broholm C, Kjems JK, Buyers WJL, Matthews PT, Palstra TTM, Menovsky AA and Mydosh JA, 1991: Phys. Rev. B **43**, 12809

Bull MJ, McEwen KA, Osborn R and Eccleston RS, 1996: Physica B **223&224**, 175

Buyers WJL and Holden TM, 1985: *Handbook on the Physics and Chemistry of the Actinides*, eds. G.H. Lander and A.J. Freeman, (North Holland, Amsterdam) Vol. 2, p. 239

Clausen KN, McEwen KA, Jensen J and Mackintosh AR, 1994a: Phys. Rev. Lett. **72**, 3104

Clausen KN, Sørensen SAa, McEwen KA, Jensen J and Mackintosh AR, 1994b: J. Magn. Magn. Mater. **140–144**, 735

Houmann JG, Rainford BD, Jensen J and Mackintosh AR, 1979: Phys. Rev. B **20**, 1105

Jensen J and Mackintosh AR, 1991: *Rare Earth Magnetism: Structures and Excitations* (Clarendon Press, Oxford)

Jensen J, McEwen KA and Stirling WG, 1987: Phys. Rev. B **35**, 3327

Jensen J, 1979: J. Phys. (Paris) **40**, C5-1

Mackintosh AR, 1985: Physica B **130**, 112

McEwen KA, Steigenberger U and Clausen KN, 1997: (to be published)

McEwen KA, Bull MJ, Eccleston RS, Hinks D and Bradshaw AR, 1995: Physica B **206&207**, 112

McEwen KA, Ellerby M and de Podesta M, 1994: J. Magn. Magn. Mater. **140–144**, 1411

McEwen KA, Steigenberger U and Martinez JL, 1993: Physica B **186–188**, 670

McEwen KA and Walker MB, 1986: Phys. Rev. B **34** 1781

McEwen KA and Stirling WG: 1981: J. Phys. C **14**, 157

McEwen KA, Stirling WG and Vettier C, 1978: Phys. Rev. Lett. **41**, 343

McEwen KA, Stirling WG and Vettier C, 1983a: Physica B **120**, 152

McEwen KA, Stirling WG and Vettier C, 1983b: J. Magn. Magn. Mater. **31–34**, 599

McEwen KA, Cock GJ, Roeland LW and Mackintosh AR, 1973: Phys. Rev. Lett. **30**, 287

Moolenaar AA, Metz A, McEwen KA, Ellerby M, Schröder-Smeibidl B and Steiner M, 1997: (to be published)

Murao T, 1971: J. Phys. Soc. Japan **31**, 683; *ibid* 1975: **39**, 50; *ibid* 1979: **46**, 40

Ott HR, Andres K and Schmidt PH, 1980: Physica B **102**, 148

Park JG and McEwen KA, 1997: (to be published)

Park JG, McEwen KA and Tasset F, 1997: (to be published)

Rainford BD and Houmann JG, 1971: Phys. Rev. Lett. **26**, 1254

Santini P and Amoretti G, 1994: Phys. Rev. Lett. **73**, 1027

Steigenberger U, McEwen KA, Martinez JL and Fort D, 1992: J. Magn. Magn. Mater. **108**, 163

Steigenberger U, McEwen KA and Kulda J, 1997: (to be published)

Walker MB, Kappler C, McEwen KA, Steigenberger U and Clausen KN, 1994: J. Phys. Condens. Matter **6**, 7365

Zochowski SW and McEwen KA, 1994: J. Magn. Magn. Mater. **140–144**, 416